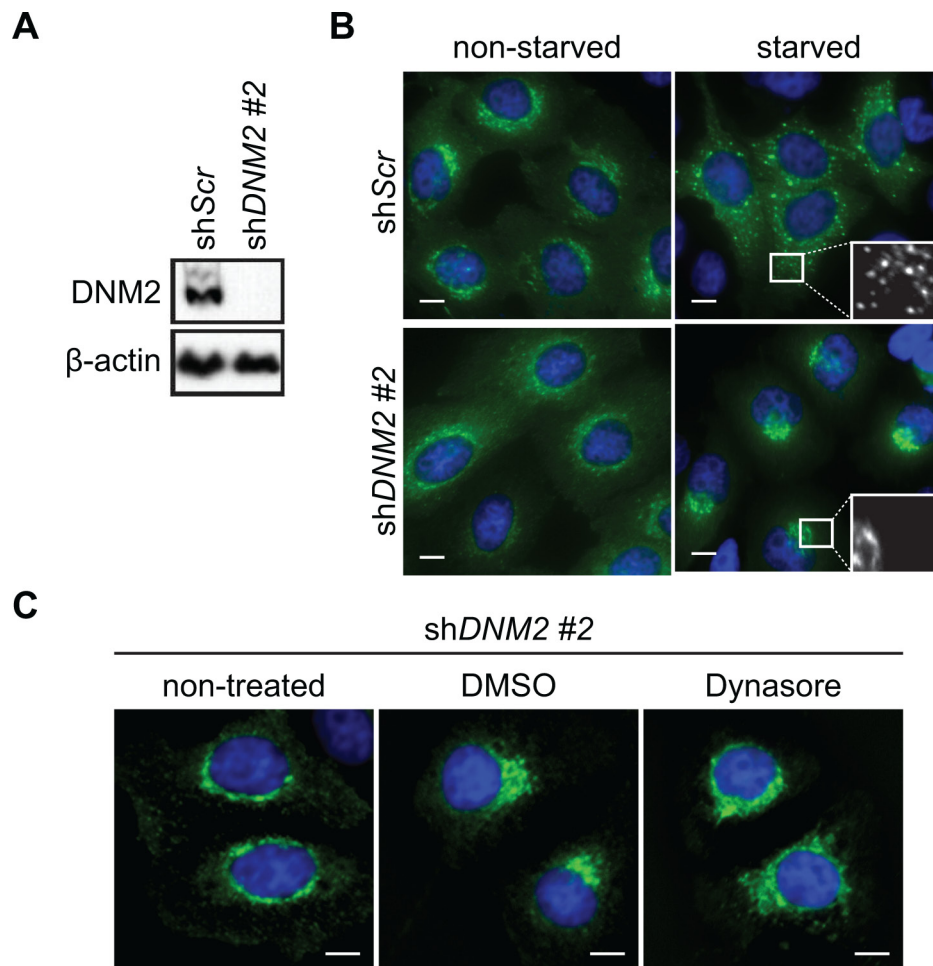


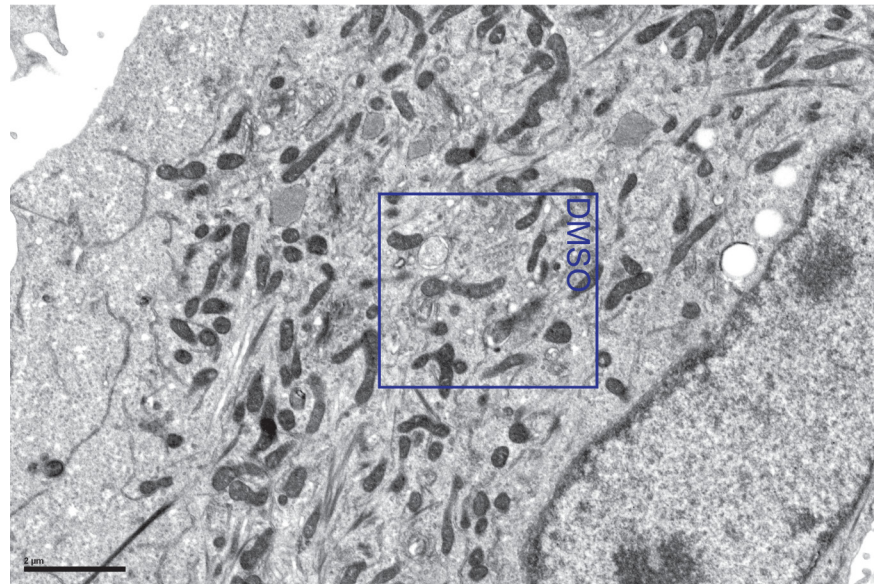
## The Bif-1-Dynamin 2 membrane fission machinery regulates Atg9-containing vesicle generation at the Rab11-positive reservoirs

### Supplementary Materials

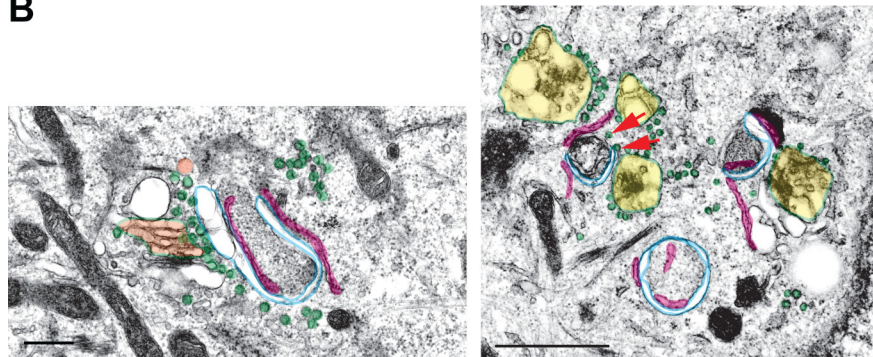


**Supplementary Figure S1: DNM2 regulates the budding of Atg9 vesicles upon nutrient starvation.** HeLa/Atg9-GFP cells were transduced with control (shScr) or shDNM2 #2 lentiviruses for 96 h. (A) Immunoblotting was performed to analyze the expression of DNM2. (B) The cells were incubated in starvation or complete medium for 1.5 h and analyzed by deconvolution fluorescence microscopy. (C) The cells were starved in the presence of 80  $\mu$ M Dynasore or control DMSO for 2 h and analyzed by deconvolution fluorescence microscopy. Scale bars represent 10  $\mu$ m.

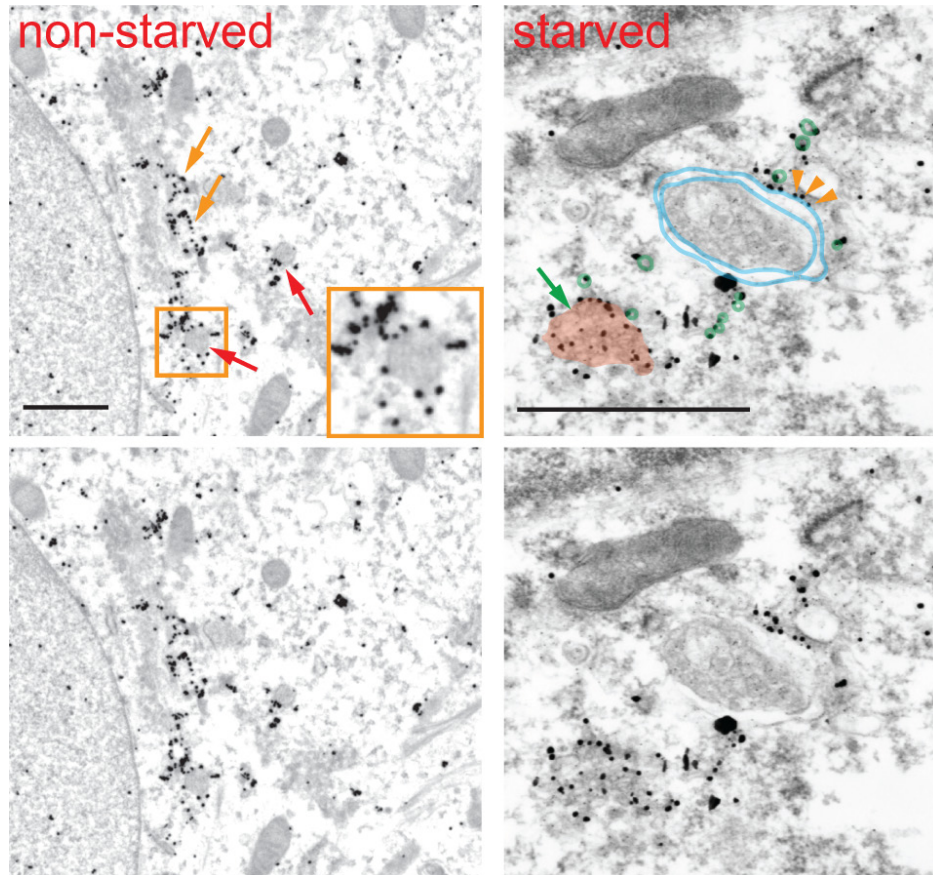
**A**



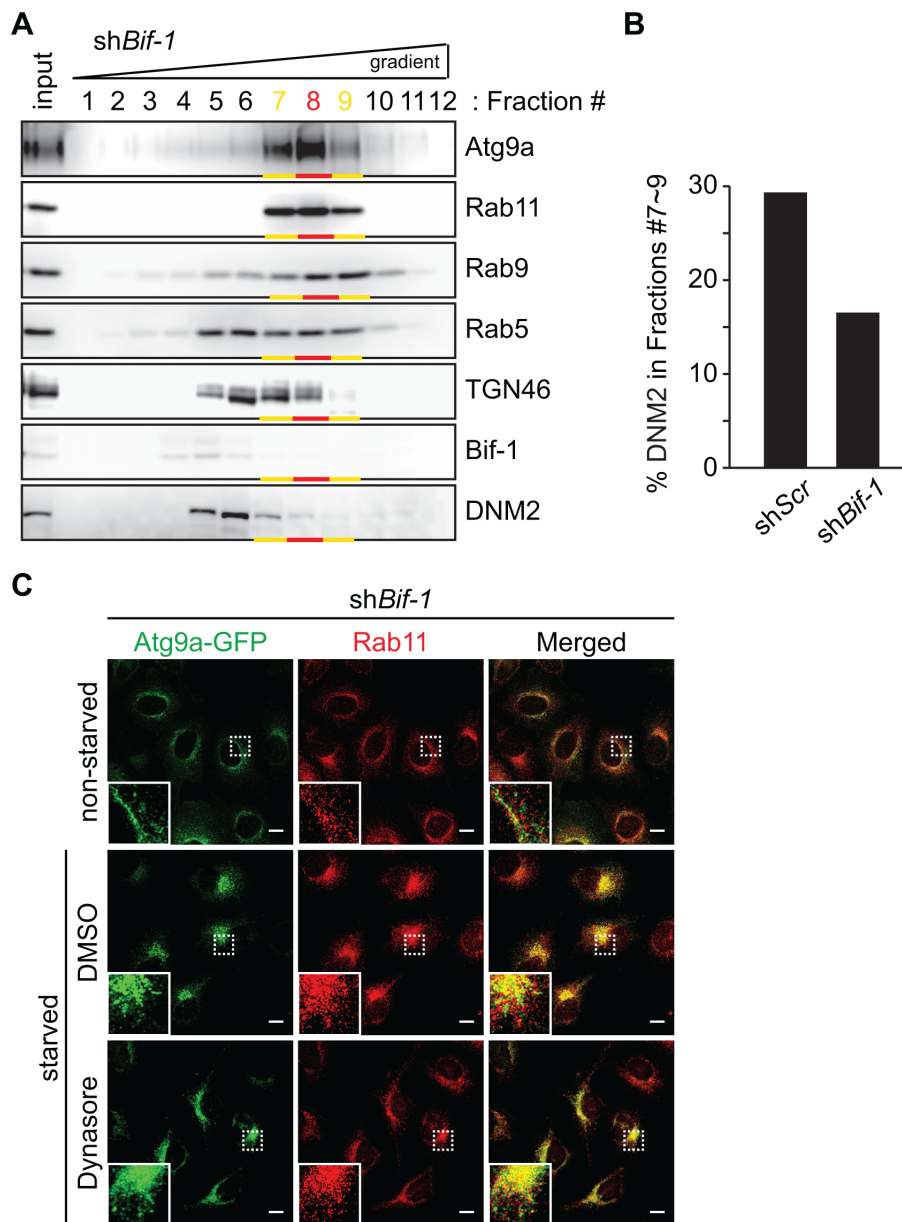
**B**



**Supplementary Figure S2: Typical immature autophagosome structures observed in starved cells.** HeLa cells were starved with control DMSO for 1.5 h and subjected to electron microscopy. A magnified image of the boxed area in (A) is shown in Figure 4. In (B) vesicular-reticular structures, resembling endosomes (yellow) or Golgi (orange), were observed nearby ER (pink)-associated immature autophagosome-like structures (blue). Vesicle-like structures were highlighted with green. Scale bars represent 2 μm.



**Supplementary Figure S3: Intracellular localization of Atg9a-GFP under non-starved and starved conditions.** HeLa/Atg9-GFP cells were incubated in complete (non-starved) or starvation (starved) medium for 2 h and subjected to immunoelectron microscopy using anti-GFP antibodies. Scale bars represent 1  $\mu\text{m}$ .



**Supplementary Figure S4: Bif-1 regulates Atg9 vesicle generation at the Rab11-positive reservoir.** (A) Post-nuclear cell homogenates prepared from Bif-1 knockdown HeLa cells were subjected to subcellular fractionation and analyzed by immunoblotting using the indicated antibodies. Similar to control HeLa cells, the majority (> 80%) of Atg9 signals were detected in Rab11-enriched fractions (Fractions #7~9). (B) The intensity of DNM2 in each fraction in A and Figure 5A were quantified by densitometry using Image Studio 5.0 software. The percentages of DNM2 fractionated into Fractions #7~10 to total DNM2 (Fractions #1~12) are shown. (C) Bif-1 knockdown HeLa/Atg9-GFP cells were incubated in complete medium or starved in the presence or absence of 80  $\mu$ M Dynasore for 1.5 h, stained for Rab11 and analyzed by confocal microscopy. Magnified images were shown in the insets. Scale bars represent 10  $\mu$ m.

**Supplementary Movie S1: A 3D surface rendered image in the boxed area in Figure 4B.**

**Supplementary Movie S2: A 3D surface rendered image in the boxed area in a Dynasore-treated cell in Figure 5B.**

**Supplementary Movie S3: 3D time-lapse movie for Figure 5C. Green, Atg9-GFP; Red, DsRed-Rab11.**